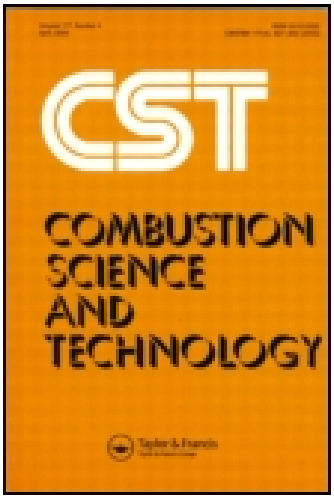

Combustion Science and Technology
Publication details, including instructions for authors and subscription information:
http://www.tandfonline.com/loi/gcst20

Universal Flame Propagation Behavior in Packed Bed of Biomass

S. Varunkumar [a] , N. K. S. Rajan [a] & H. S. Mukunda [a]
[a] Combustion Gasification and Propulsion Laboratory, Department of Aerospace Engineering , Indian Institute of Science , Bangalore , India
Accepted author version posted online: 20 Mar 2013.Published online: 25 Jul 2013.

To cite this article: S. Varunkumar , N. K. S. Rajan & H. S. Mukunda (2013) Universal Flame Propagation Behavior in Packed Bed of Biomass, Combustion Science and Technology, 185:8, 1241-1260, DOI: 10.1080/00102202.2013.782297

To link to this article: http://dx.doi.org/10.1080/00102202.2013.782297

Combust. Sci. Technol., 185: 1241–1260, 2013

ISSN: 0010-2202 print/1563-521X online
DOI: 10.1080/00102202.2013.782297

Taylor & Francis
Taylor & Francis Group

UNIVERSAL FLAME PROPAGATION BEHAVIOR IN PACKED BED OF BIOMASS

S. Varunkumar, N. K. S. Rajan, and H. S. Mukunda
Combustion Gasification and Propulsion Laboratory, Department of Aerospace Engineering, Indian Institute of Science, Bangalore, India

This article aims at seeking the universal behavior of propagation rate variation with air superficial velocity (V_s) in a packed bed of a range of biomass particles in reverse downdraft mode while also resolving the differing and conflicting explanations in the literature. Toward this, measurements are made of exit gas composition, gas phase and condensed phase surface temperature (T_g and T_s), and reaction zone thickness for a number of biomass with a range of properties. Based on these data, two regimes are identified: **gasification**—***volatile oxidation accompanied by char reduction reactions up to 16 ± 1 cmls of V_s and above this, and*** **char oxidation**—***simultaneous char oxidation and gas phase combustion. In the gasification regime, the measured T_s is less than T_g; a surface heat balance incorporating a diffusion controlled model for flaming combustion gives $T_s = 482[K]Nu_0^{0.36}$ and matches with the experimental results to within 5%. In the char oxidation regime, T_g and T_s are nearly equal and match with the equilibrium temperature at that equivalence ratio. Drawing from a recent study of the authors, the ash layer over the oxidizing char particle is shown to play a critical role in regulating the radiation heat transfer to fresh biomass in this regime and is shown to be crucial in explaining the observed propagation behavior. A simple model based on radiation–convection balance that tracks the temperature–time evolution of a fresh biomass particle is shown to support the universal behavior of the experimental data on reaction front propagation rate from earlier literature and the present work for biomass with ash content up to 10% and moisture fraction up to 10%. Upstream radiant heat transfer from the ash-laden hot char modulated by the air flow is shown to be the dominant feature of this model.***

Keywords: Ash effect; Char oxidation; Gasification; Universal flame propagation behavior

1. INTRODUCTION

Countercurrent packed bed combustion is a widely studied configuration for the thermochemical conversion of biomass with applications in medium scale heating, power generation, and more recently in domestic cooking (Dasappa et al., 2003; La Fontaine and Reed, 1993; Mukunda et al., 2010; Porteiro et al., 2010a; Saastamoinen et al., 2000; Thunman and Leckner, 2005; Yang et al., 2004;). Two phases of conversion are observed in the consumption of the biomass (see for instance, Varunkumar et al., 2011). The first phase involves the evolution of volatile gases and conversion of

Received 8 May 2012; revised 1 March 2013; accepted 1 March 2013.
Address correspondence to S. Varunkumar, Combustion Gasification and Propulsion Laboratory, Department of Aerospace Engineering, Indian Institute of Science, Bangalore, India. E-mail: varunsivakumar@gmail.com

the biomass to char with a distinct flame front propagating through the bed. This is referred to as the flaming mode or the ignition propagation phase. Once the front reaches the grate, all biomass is devolatilized, and an amount of hot char up to 20% depending on the air flow rate (Ryu et al., 2006; Yang et al., 2004;) is left on the grate. This leftover char undergoes surface oxidation with the incoming air and generates primarily CO and CO_2 and a little H_2. Carbon dioxide so generated passes through the hot char on top and can undergo reduction with carbon to form CO. This is the second phase and is referred to as the *char mode*. At least 70% of the biomass is consumed in the first phase, and hence propagation of flame front through a packed bed during the flaming mode has received greater attention in the past two decades (see for instance, Porteiro et al., 2010a; Saastamoinen et al., 2000; Thunman and Leckner, 2005; Yang et al., 2004).

2. EARLIER EXPERIMENTS AND MODELS

Superficial velocity (V_s) has been identified as the most influential parameter affecting the fuel mass flux ($\dot{m}_f$) (see Figure 1), bed temperature (T_b), and exit gas composition (Fatehi and Kaviany, 1994; Reed et al., 1999); the other parameters affecting the conversion process are density, moisture content, ash content, particle size and shape of biomass, and the bed porosity. The data on propagation rate ($\dot{r}$) and bed temperature (T_b) are reported in several studies. All the experiments use the data from thermocouple inserted into the bed from the wall to obtain the propagation rates. Essentially, the rise in temperature up to a significant value (say, 750 K) is counted as the arrival of a propagation front, and the distance between the thermocouple locations divided by the time of travel of the high temperature wave is taken as the propagation rate. The thermocouple used in these experiments is also an issue in the elucidation of the propagation process. While Fatehi and Kaviany (1994) use *B*-type

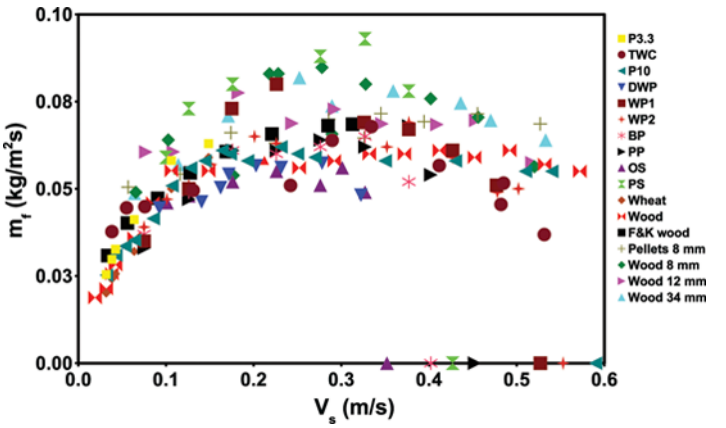

Figure 1 Fuel consumption rate ($m_f = \rho_p \dot{r}$) with air superficial velocity. P3.3 – pellets (3.3% ash), P10 – pellets (10% ash), Wh – wheat, Wo – wood, from current work. *WP*1, *WP*2, *BP*, *PP*, *OS*, PS – Porteiro et al. (2010a). F&K – Fatehi and Kaviany (1994), P8 – pellets 8 mm, *W*8, *W*12, *W*34 – wood 8 mm, 12 mm, 34 mm – Ronnback et al. (2001). DWP – digester waste pellets – Gnanendra et al. (2012). TWC – Horttanainen et al. (2002). (Figure is provided in color online.)

enabling capture of high temperatures (up to 2000 K), Thunman and Leckner (2005), Saastamoinen et al. (2000), Yang et al. (2004), and Porteiro et al. (2010a) use *K*-type, which prevents them from obtaining temperatures beyond 1500 *K* with consequences of possible misinterpretation of the true thermal behavior of the bed. In this work, *R*-type thermocouples are used (upper limit 1900 K).

Fatehi and Kaviany (1994) have done experimental as well as modeling studies to bring out the effect of superficial velocity (V_s) on fuel mass flux ($\dot{m}_f$) and bed temperature (T_b). By assuming that the reaction front thickness (δ_f) is large compared to the particle diameter (d), a volume averaged pseudo-homogeneous 1-D model (see Dosanjh et al., 1987; Gort, 1995) is developed by them. By treating the propagating front as analogous to a premixed flame they have used classical asymptotic analysis with the limitation of treating diffusion controlled rates in terms of activation energy for mass diffusion. The model results are shown to agree well with the experiments for certain choice of parameters, and it is stated that the results are most sensitive to the choice of kinetic constants. If the principal idea of reaction control were true, the propagation rates would show strong dependence on the nature of biomass because the kinetic data are strongly dependent on the presence of elements such as sodium and potassium, which are naturally present in widely differing proportions. This is not true, as shown by other experimental data and the data analysis to be presented subsequently.

Porteiro et al. (2010a) report experimental results of fuel mass flux ($\dot{m}_f = \rho_p \dot{r}$, ρ_p being the packing density of the bed) and T_b variation for the entire range of V_s (up to extinction) for eight different types of biomass. A K-type thermocouple was used in their work to obtain $\dot{r}$ and $\dot{m}_f$. Gort (1995) reports experimental results for $\dot{r}$, T_b, and exit gas composition (CO, CO_2, O_2 and C_xH_y only) for 10 mm wood samples with 10% moisture as a function of V_s. Similar experiments have been performed by Ronnback et al. (2001). Experimental results from all these works are compiled with appropriate corrections to account for varying ash and moisture content to bring out the universal behavior of propagation rate variation with superficial velocity (see Section 3.2). Additional experiments were performed to measure gas phase and condensed phase temperature and O_2 drop across the flame front, hitherto not reported elsewhere. These measurements are shown to mark transition points based on physical and chemical processes leading to a new viewpoint on the classification of operating regimes.

The influence of other fuel-related parameters such as density, particle size, moisture content, etc., have been studied using experiments and modeling (see for instance Gort and Brouwers, 2001; Johansson et al., 2007; Ronnback et al., 2001; Yang et al., 2004). By using wood pieces of 8, 12, and 34 mm, Ronnback et al. (2001) show that there are no perceptible differences beyond experimental errors. Ryu et al. (2006) experimentally investigated the effect of fuel type, equivalence ratio, and particle size on the fixed bed combustion of biomass in the range $V_s = 6$–11 cm/s. That the ignition front speed is inversely proportional to bulk density observed by Ryu et al. (2006) and Saastamoinen et al. (2001) is considered somewhat surprising, even though this follows simply from the surface heat balance condition (see Quintiere, 2006; Varunkumar et al., 2011).

The effect of ash has had relatively little attention compared to other fuel-related parameters. It appears from the literature that only Cooper and Hallett

(2000) and Ryan and Hallett (2002) have incorporated the effect of ash by modifying the heat and mass transfer coefficients and the effective thermal conductivity (that includes radiation), as Varunkumar et al. also did (2011) recently. The present work takes into account the effects of ash and shows that the temperature dependence of emissivity of ash is crucial in explaining the observed behavior. Saastamoinen et al. (2001) have built upon their earlier work (Saastamoinen and Richard, 1996; Saastamoinen et al., 2000) a model for propagation of the ignition front. The principal issue with this model is that most of the information in the model arises out of experimental data, reducing the possible predictive capability.

Recently Collazo et al. (2012) have explored a three-dimensional model to explain the features of packed bed combustion. The model is complex and invokes kinetics for a char–oxygen reaction. The temperature–time profiles are much sharper in the experiments compared to predicted ones. That the reason for this could be a near-diffusion control of the process and that their assumed kinetic influence would perhaps have been unrealistically stronger is not recognized in the work.

In summary, the key issues that have remained unaddressed are as follows: (a) the differences in perception of the behavior of the packed bed in different zones, (b) the implication that there are significant differences in the propagation rate between various fuels, and (c) the essential features of a model to reconcile the data seeking possible universality of the behavior and to propose a prediction procedure for the propagation rate with justifiable inputs. It is also important to explore a one-dimensional model that captures as many experimental features as feasible. These are considered below.

3. EXPERIMENTS ON A STEEL AND GLASS TUBE REACTORS

The experiments consisted of two parts. The first part of the experiments was done in a 100 mm diameter insulated stainless-steel reactor and involved measurement of overall bed parameters including fuel consumption rate ($\dot{m}_f$), bed temperature (T_b), and exit gas composition. These were conducted at eight different superficial velocities from 5.5–26.5 cm/s. Apart from this, experiments were conducted in both steel and transparent reactors up to a superficial velocity of 70 cm/s to determine the extinction conditions. The experiments at lower values of V_s are aimed at applications to domestic stoves; at these low velocities, the exit velocities of hot combustion gases also will be low and this helps limit the particulate carryover (see Mukunda et al., 2010). The larger values of V_s are relevant for combustion of these fuels in furnaces for boilers. The bed temperature, T_b, was measured with 0.4 mm R-type thermocouples at specific intervals along the length of the stove (three at 30 mm spacing). The exit gas composition was measured with a Maihak analyzer (for CO, CO_2, H_2, CH_4, and O_2) using a probe located about 10 mm above the bed; the response time is large—about 4 mins.

The second part of the experiments was performed in a 100 mm transparent reactor, and it involved measurement of gas-phase and condensed-phase temperature (T_g and T_s) with the help of 100 μm R-type thermocouples, reaction zone thickness (δ_f) from the visual data, and coupled measurements of O_2 fraction and temperature at a fixed point. Toward this, a gas sampler of 2.5 mm dia and a 1 mm dia K-type thermocouple were positioned close to each other to detect the changes as the flame front moved past this point. The sensor used is a Lambda sensor that provides

Table 1 Properties of biomass used

Item	Wood chips	Pellets	Wheat	Thin wood chips
ρ_p, kg/m^3	615	1260	1200	350
Size, *mm*	$10 \times 10 \times 15$	6 dia, 15 length	4 (average)	$12 \times 12 \times 4$
ρ_b, kg/m^3	462	794	1000	300
% Ash	1	10	1	1
% Moisture	10	6 - 10	6	10
CHO	$CH_{1.7}O_{0.79}$	$CH_{1.62}O_{0.93}$	$CH_{1.3}O_{1.1}$	$CH_{1.7}O_{0.79}$
A/F_s	5.2	4.5	3.6	5
% Volatiles	87	81	80	80

A/F_s = Stoichiometric air-to-fuel ratio; ρ_p - particle density; ρ_b - packed bed density.

a voltage output corresponding to the amount of O_2 present in the gases. The sensors are calibrated using gases containing 0% and 21% O_2. The response is linear in this regime, and the total response time is composed of the time of transport of sample to the sensor of 10 s and the sensor response time of <0.5 sec. The choice of these sizes accounted for the conversion time of $\sim$100 s for a 10 mm particle size.

Wood, agro-residue pellets, wheat, and thin wood chips covering a wide range of size, shape, and density were used (see Table 1) as fuels. This choice was made as follows: wood pieces and thin chips help replicate earlier experimental data; agro-residue pellets have a high ash content; and wheat is very dense and small in size and hence offers a variant in the list of fuels used.

Most experimental details are available in Varunkumar et al. (2011). The points to be emphasized are that $\dot{r}$ measurements are made using thermocouples introduced into the bed from the wall and weight loss measurement as well. The $\dot{r}$ from both these approaches matched as long as the fuel was dense and did not have sharp edges. When thin wood chips or flakes were used, the $\dot{r}$ measured using thermocouples was larger than that from the weight loss method (by 20–30 %). Visual observation of the propagation behavior in the transparent reactor showed that for dense fuels, the propagation occurred after each layer lost its volatiles and entered the char conversion condition, but with flakes and sharp edged fuels, the jump occurred even when all the layer had not lost its volatiles. This is related to the mass to be heated for ignition. Sharp-edged flakes with individual mass being lower will ignite faster compared to others; ignition of the subsequent layer occurs even without proper consumption of the current layer.

4. EXPERIMENTAL RESULTS

Mass loss with time for wood for different air flow rates is shown in Figure 2, and two distinct phases of conversion, namely, *flaming* and *char* mode can be discerned. In the flaming mode, the *average slope* calculated from the mass loss curve, neglecting the start-up phase of the initial 100 s, is a measure of the fuel consumption rate. It is clear that the fuel burn rate increases with increase in air flow rate. Also the amount of char left behind at the end of the flaming mode decreases with increased air flow rate (and so, V_s).

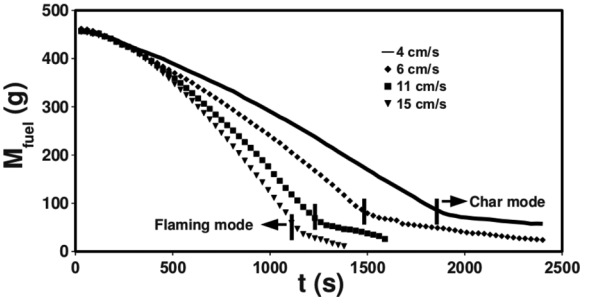

Figure 2 Mass loss vs. time of wood for different air superficial velocities.

4.1. Compiled Propagation Rate

Figure1 shows the propagation rate for 16 types of biomass obtained from literature along with the experimental results of the current work. The data show a universal trend: If we allow for experimental uncertainties, including the moisture content totaling to about 5%, it appears that the plot can be taken to be represented by a single curve with propagation rate increasing with superficial velocity up to about 16 cm/s and then saturates. But this data required correction because of two issues, one related to the fuel consumption rate measurement method and the other related to the variation in the ash and moisture fraction of the fuel used. These issues are explained in the following paragraphs.

4.1.1. Mass loss measurement method. An important point to be emphasized is that in the current study $\dot{r}$ measurements is made using thermocouples introduced into the bed from the wall (Method 1) and weight loss measurement as well (Method 2). The fuel burn rate increases with increase in air flow rate in the range shown (Figure 2).

The $\dot{r}$ from both these approaches matched as long as the fuel was dense and did not have sharp edges. When thin wood chips or flakes were used, the $\dot{r}$ measured using thermocouples was larger than that from weight loss method (by 20 to 30%) as shown in Figure 3. For wood and wheat, the propagation rates obtained from the two methods matched. But for thin wood flakes, which has sharp edges compared to wood and wheat, propagation rate measured using Method 1 is at least 20% greater than the results obtained from Method 2. As observed earlier, this is related to the thermal inertia of the biomass particle ($\rho c_p \Delta T$). This is reflected in the difference in flaming to ignition time ratio; for thin wood flakes it is 5 and for dense biomass it is 2.

4.1.2. Correction for ash and moisture content variation. The fuel consumption rate is also influenced by the presence of inerts (ash) and moisture. The inerts remain in the condensed phase and contribute to absorption of heat. The heat release in the gas phase is reduced by the fraction of inerts. Moisture in the condensed phase draws energy for both sensible enthalpy rise and evaporation. The vapor will get heated up to the flame temperature in the gas phase and reduce the peak temperature. Since both ash and moisture contribute to reduction in propagation rate, it was thought that they be correlated in terms of $\rho_p \dot{r}(1 + \alpha f_{ash} + \beta f_w)$, where ρ_p, f_{ash}, and f_w

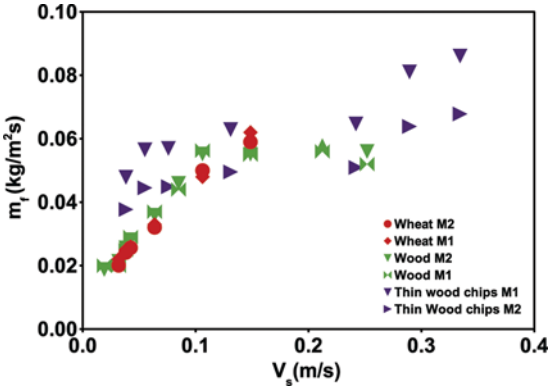

Figure 3 Propagation rate estimated from two methods; M1 - method 1; M2 - method 2; note that thin wood chips show larger regression rate compared to dense biomass - wood and wheat. (Figure is provided in color online.)

are the density of the biomass, ash fraction, and moisture fraction in the biomass, respectively. The coefficients α and β are introduced here because the enthalpy absorbed by inerts and moisture may acquire different values; both are set to 1 here. This choice is justified by the following observation from model calculations presented later—the moisture fraction in the biomass considered as normal is about 10% since it constitutes the equilibrium moisture that biomass acquires to within $\pm 2\%$ when the biomass is allowed to dry in a covered ambient atmosphere. Moisture fractions lower than this value add additional heat, and larger values imply additional loss of enthalpy due to evaporation. For energetic applications, one would not deviate from this value by more than 10%. The effective specific heat of the particle deviates from that of sun-dry biomass only during heat up from ambient temperature to 373 K and the time for heat up is only about 20% of the total ignition time. After vaporization, the effective specific heat is that of the biomass and the time spent is about 60% of the total time for ignition. From Saastamoinen and Richard (1996) and Thunman et al. (2004), it is clear that the drying and devolatilization processes can overlap, thereby bringing down the effect of specific heat variations further. In light of these features, the fact that $\beta = 1$ leads to collapse of most of the data on propagation rate vs. air flow rate into a single curve independent of biomass type is considered adequate justification for the choice of β.

$$m_{fc} = \rho_p \dot{r}_c = \rho_p \dot{r}_m (1 + \alpha f_{ash} + \beta f_w),\ \alpha = 1,\ \beta = 1 \tag{1}$$

where m_{fc} is the corrected fuel mass flux, $\dot{r}_c$ is the corrected propagation rate, and $\dot{r}_m$ is the measured propagation rate. The corrected data from all the available sources (Fatehi and Kaviany, 1994; Horttanainen et al., 2002; Porteiro et al., 2010a Ronnback et al., 2001) and from the present work are shown in Figure 4.

Figure 4 shows that with the incorporation of the corrections, the scatter in the data has come down, and the variation of fuel mass flux with V_s is nearly independent of the biomass used within the experimental limitations. Extinction occurs

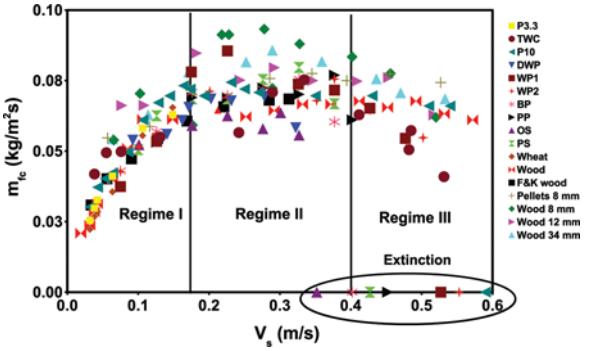

Figure 4 Corrected fuel consumption rate variation with superficial velocity. (Figure is provided in color online.)

at around 55 cm/s with a sharp drop in $\dot{m}_f$ for all the fuels used in this study. Experimental results of Porteiro et al. (2010a) show extinction limits for some fuels being as low as 35 cm/s. Experiments conducted to explore the possible causes at high V_s showed that the extinction velocity depended on the rate at which V_s is raised. It was found important to make sure that at least a couple of hot char layers are formed before the air flow can be increased to beyond 30 cm/s. Gradual increase in V_s in small steps led to extinction at ~55 cm/s for all fuels used in present experiments. It is therefore inferred that observed extinction speeds lower than this value must be an artifact of the experimental procedure. This view is also supported by the work of Fatehi and Kaviany (1994).

4.2. Existing Classifications of Operating Regime

Figure 5 shows the three major classifications of propagation regimes. Fatehi and Kaviany (1994) classified the operating regimes into a oxygen limited fuel rich part (regime I and II in Figure 5) and a fuel limited fuel lean part (regime III in

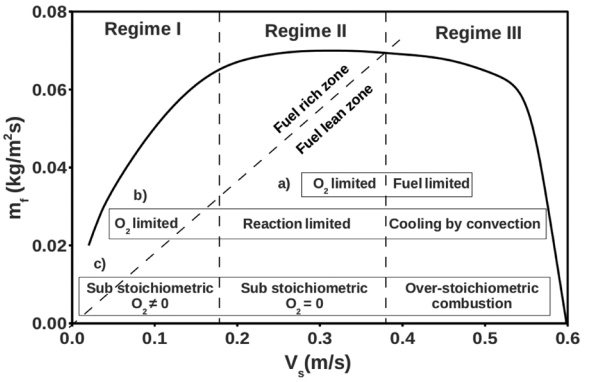

Figure 5 Classification of operating regimes in packed bed combustion: (a) Fatehi and Kaviany (1994), (b) Ronnback et al. (2001), (c) Porteiro et al. (2010a).

Figure 5). Porteiro et al. (2010a) classified the operating regime into three sections, namely, *fuel-rich oxygen limited* combustion up to $V_s = 17\,\text{cm/s}$ (regime I in Figure 5), *fuel-rich fuel limited* combustion up to 35 cm/s (regime II), and a *convective cooling dominated* region beyond 35 cm/s (regime III). Though this classification is claimed to be an extension of that of Fatehi and Kaviany (1994), the idea of fuel rich fuel limited zone used here appears incorrect; there is no such regime in Fatehi and Kaviany (1994). There are also difficult-to-justify char stoichiometry ideas in Porteiro et al. (2010a). This issue is discussed later. The classification of Gort (1995) is similar to that of Porteiro et al. (2010a), except that the regime I is titled *partial gasification* since some char is left behind in the process.

Ronnback et al. (2001) propose a different classification. The classification proposed has three regimes, namely (i) *substoichiometric combustion with incomplete consumption of oxygen* in regime I, (ii) *substoichiometric combustion with complete consumption of oxygen* in regime II, and (iii) *over-stoichiometric* combustion from a superficial velocity of about 40 cm/s. Their conclusion (i) is based on a short duration oxygen data over the bed (~4 mins) with instruments whose response time is comparable (more on this issue later).

4.2.1. Air-to-fuel ratio and char yield variation with V_s. Figure 6 shows the air-to-fuel ratio (A/E) variation and amount of char left at the end of flaming mode as percentage of the initial mass with superficial velocity estimated from the air flow rate and fuel consumption rate presented in Figure 1.

Air-to-fuel ratio increases with increase in superficial velocity. Stoichiometric A/F is attained at $V_s = 38\,\text{cm/s}$ and matches with the experimental results from other studies shown in Figure 1. An important point to note is that the char left over after the flame front reaches the grate decreases from 18% at 5 cm/s to almost zero at 22 cm/s. Implications of increase in A/F combined with decrease in char left over on elucidating the processes in the flame front propagation through the bed will be brought out later.

4.3. Exit Gas Composition

Figure 7 shows the exit gas composition measured for pellets over a range of V_s. Data for wood and other fuels used in the current work and that of Gort

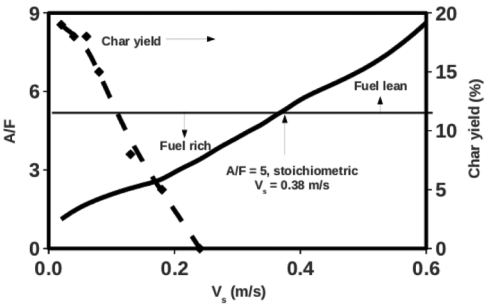

Figure 6 A/F and char yield variation with superficial velocity.

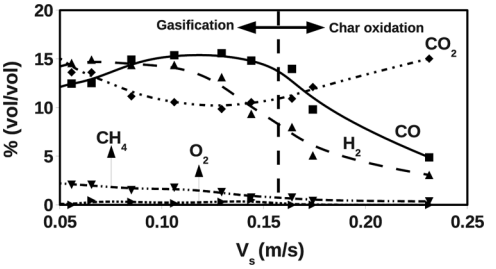

Figure 7 Variation of exit gas composition with superficial velocity.

(1995) also show a similar trend. Both CO and H_2 are at reasonably high levels between 10–16% up to a V_s of about 16 cm/s and drop subsequently. CH_4 is around 2.5% at low V_s and drops continuously through 16 cm/s. CO_2 goes up through $V_s = 16$ cm/s. O_2 remains very negligible throughout with below measurable levels beyond 16 cm/s. From these observations, it appears that $V_s = 16$ cm/s marks a transition point. More evidence to this transition will be presented subsequently.

The plot shows little O_2 throughout the range of V_s, and it can therefore be concluded that the operation is substoichiometric. Exit gas composition data of Gort (1995) show significant amount of O_2 in the exit gas (~5%) only at $V_s = 50$ cm/s and therefore even beyond 25 cm/s the operation is substoichiometric. This is also supported by the fact that the amounts of H_2 and CO are not very low. To further explore how O_2 is depleting through the bed, it was thought important to use a sensor with a better response time than the Maihak analyzer (response time is around 4 min). Hence, a λ sensor with a response time of < 10 s was used to measure the O_2 drop across the reaction zone. The data obtained from the simultaneous output of the λ sensor and the thermocouple with time are set out as a cross-plot between them in Figure 8. These show that for all the cases considered, the O_2 fraction transitions sharply with temperature (to be emphasized later).

A simultaneous visual examination (including video) showed that this occurred as soon as there was a streak of gaseous flame past the measurement point (sample videos are posted at http://cgpl.iisc.ernet.in/videos) up to $V_s = 16$ cm/s, and beyond this the drop coincided with the ignition of char surface.

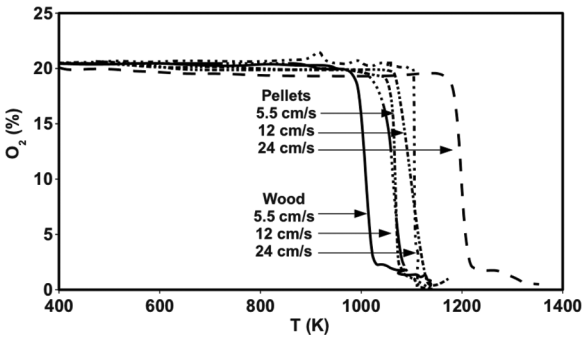

Figure 8 O_2 drop as a function of temperature increase across the propagating flame front.

4.4. Gas-Phase vs. Condensed-Phase Temperature

Figure 9 shows gas phase, condensed phase, and peak bed temperature measured in the superficial velocity range of 5–26 cm/s. Reaction zone thickness (δ_f) is set out in terms of the number of particle depths. The error bar on δ_f is larger at smaller thickness because it is not possible to distinguish below one particle size thickness.

Gas phase temperature (T_g) is constant (1600 K) up to about a V_s of 17 cm/s. It is important to note that in this range of V_s, the A/F increases from 1.5 to 2.7 (see Figure 6). This is a clear indication of diffusion flame behavior because any level of premixing should lead to a corresponding increase in gas phase temperature with the A/F moving toward stoichiometry. Also the fact that the condensed phase surface temperature (T_s) is less than T_g is a feature observed in diffusion flame surrounding the devolatalizing particle similar to single particle combustion. T_s increases from 973 K to 1600 K as V_s is increased from 5 cm/s to 17 cm/s. Visual observation showed that the biomass particle undergoes loss of volatiles with a flame surrounding it. This, combined with the fact that the O_2 drops from 21% to 0% within one particle depth, shows that the char left behind by the ignition front participates only in reduction reactions with CO_2 and H_2O. Therefore this regime is classified as *gasification dominated.*

Beyond 17 cm/s, measured values of T_g and T_s were equal and same as the peak bed temperature. Therefore, only T_{pb} is reported for $V_s > 17$ cm/s. At $V_s = 17$ cm/s, the measured T_{pb} is 1600 K and increases with further increase in V_s. As was shown earlier, the maximum temperature attainable in the gas phase when there is no oxygen access to char surface is 1600 K. So measured temperatures of more than 1600 K for $V_s > 17$ cm/s show that the char participates in oxidation reactions. Visual examination in this regime showed that the gas phase flame of volatiles generated from the fresh biomass gets blown off because of high local velocities, and the unburned volatiles burn above the devolatalizing layer biomass along with the hot char layer. Experiments with single particles in a stream of air showed that

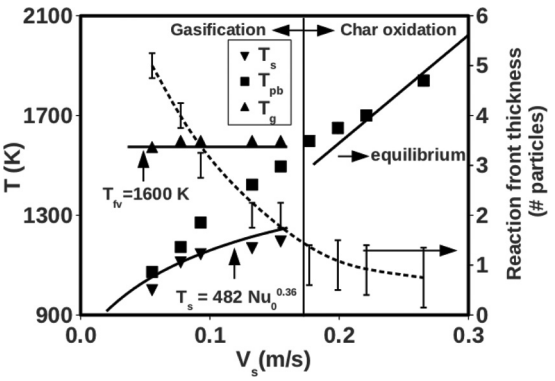

Figure 9 Variation of gas, surface, and peak bed temperatures (T_g, T_s, T_{pb}), reaction zone thickness with V_s. Solid lines - $T_s = 482[K]Nu_0^{0.36}$ (model) in the gasification regime and equilibrium temperature in char oxidation regime and volatiles flame temperature (T_{fv}) = 1600 K in gasification regime. Data points are from experimental results. Dotted line represents the mean behavior of reaction zone thickness, δ_f.

the volatile flame surrounding the single particle gets blown off at a Reynolds number of around 100 [$Re = Vd/\nu$, V is the free stream velocity (m/s), d is particle diameter (10–15 mm), and ν is kinematic viscosity of air (m^2/s)]. This occurs in a bed at a Reynolds number of around 150 [$Re_{bed} = V_s d/\nu(1-\phi)$, V_s is the superficial velocity (m/s), d is diameter of single fuel particle (10–15 mm), and ϕ is the bed porosity = 0.3]. The Reynolds number at which volatiles flame blow off is slightly higher in the case of bed, understandably because of the better thermal environment compared to a single particle in ambient stream.

Also, since the gas-phase reactions are faster than the condensed-phase surface reactions, participation of char in oxidation can only mean that stoichiometry is reached in the gas phase at around $V_s = 17$ cm/s and it becomes lean beyond this superficial velocity. This also shows that the claim of Porteiro et al. (2010b) based on air excess ratio scaling using char fraction and char stoichiometric A/F that char stoichiometry is attained at $V_s = 17$ cm/s is inconsistent with this observation. Conditions at $V_s = 17$ cm/s are closer to attainment of volatile stoichiometry, and scaling the air excess ratio with volatile fraction in biomass and volatile stoichiometric A/F instead of values corresponding to char led to a value of 1 for air excess ratio. So the conclusions of Porteiro et al. (2010b) are coincidental, and the actual conditions are closer to attainment of volatile stoichiometry at $V_s = 17$ cm/s.

These features, combined with the fact that the gas-phase and condensed-phase temperatures are equal, imply *simultaneous oxidation of volatiles and char*. This is the reason for very little char left at the end of flaming mode beyond $V_s = 17$ cm/s (see Figure 6). This regime is termed *char oxidation dominated*. The reaction zone in this regime is like a stirred reactor with heterogeneous surface reactions. Since the dominant process is char surface reaction and is controlled by diffusion of oxygen to the surface, this regime is also *diffusion controlled*.

From the videos taken at various values of V_s, two typical conditions of the bed (at $V_s = 7$ and 20 cm/s) have been described in Figure 10. At low V_s, δ_f is many particles deep. At high V_s, it reduces to one particle depth. An interesting feature of this behavior is that $\delta_f V_s$ is constant for the range of data shown ($27 \pm 3\ cm^2/s$), a feature similar to what is observed in premixed flames. This should not be taken to imply that premixed flame theory will describe the processes, because the thermochemical dynamics involves diffusion limitedness significantly as discussed earlier. Also for $V_s < 17$ cm/s, ignition occurs in the gas phase and the ignition temperature is around 650 K. For $V_s > 17$ cm/s, the volatiles are convected up and the char surface ignites the volatiles, implying that the char surface ignites first and therefore the ignition temperature is

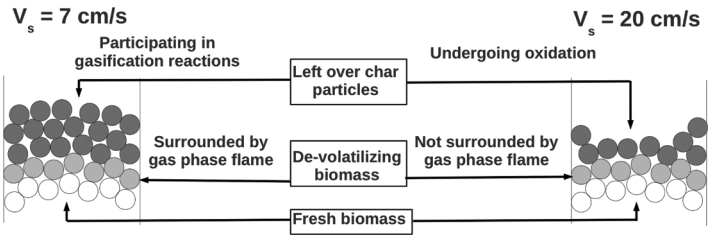

Figure 10 Schematic of the reaction zone at $V_s = 7$ cm/s and 20 cm/s.

around 850 K. This is the reason for the 200–300 K difference in the temperature at which O_2 drop from 21% to 0% between 12 cm/s and 24 cm/s (see Figure 8).

4.5. Classification of Operating Regime

Using the experimental data shown until now, the operating regime can be classified into *gasification dominated* for $V_s < 17$ cm/s and *char oxidation dominated* for $V_s > 17$ cm/s. Characteristic features of these regimes are given below.

4.5.1. Gasification dominated regime.

1. CO and H_2 in the exit gas composition are both 15% (see Figure 7).
2. Gas-phase temperature remains constant at 1600 K even though A/F increases from 1.5 to 2.7 as V_s is increased from 5 cm/s to 17 cm/s (see Figure 9).
3. Condensed-phase temperature increases from 973 K to 1600 K as V_s is increased from 5 cm/s to 17 cm/s (see Figure 9).
4. It is inferred from the last two points combined with visual examination that in this regime, the devolatilizing biomass particle is surrounded by a flame similar to a single particle.
5. The reaction zone thickness is 5–6 particles deep at $V_s = 5$ cm/s and drops to 1–2 particles deep at 17 cm/s (see Figure 9).
6. Lambda sensor data combined with visual examination shows O_2 drops from 21% to 0% within one particle depth (see Figure 8). This feature, combined with the presence of diffusion flame around the particle, indicates that all the incoming O_2 is consumed by the volatiles and the surface of the devolatalizing particle as well as the char left over above the ignition front do not have access to oxygen. Hence they participate only in reduction of CO_2 and H_2O and so the regime is termed *gasification dominated*.

4.5.2. Char oxidation dominated regime.

1. CO and H_2 drop sharply to less than 10% with a corresponding increase in CO_2 fraction as V_s is increased beyond 17 cm/s (see Figure 7).
2. Gas-phase temperature and condensed-phase surface temperatures are equal and match closely with the equilibrium temperature corresponding to the A/F (see Figure 9).
3. $T_g > 1600K$ in this regime indicates attainment of gas phase stoichiometry and beginning of char oxidation.
4. This combined with the fact that the reaction zone is just 1–2 to particles deep (see Figure 9) indicates simultaneous oxidation of volatiles and char.
5. In this regime O_2 also drops from 21% to 0% within one particle depth (see Figure 8). This, combined with close agreement of bed temperature with equilibrium temperature, indicates that the reaction zone resembles a stirred reactor with heterogeneous surface reaction of char. Diffusion controlled nature of char oxidation makes the dynamics transport controlled in this regime as well.
6. Participation of char in oxidation reaction and its importance in causing ignition of the volatiles justifies classifying this regime as *char oxidation dominated*.

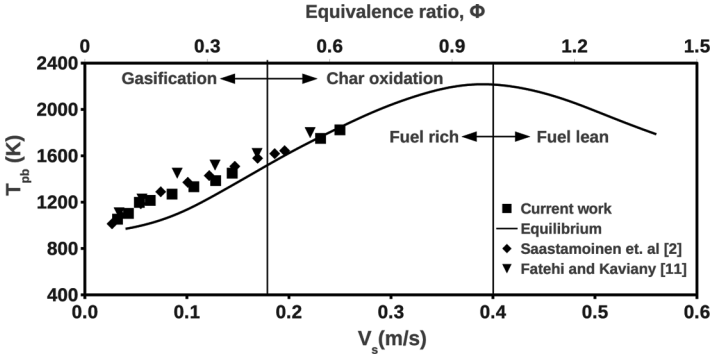

Figure 11 Bed temperature with V_s from the current work, Fatehi and Kaviany (1994), Saastamoinen et al. (2000), and equilibrium calculations.

4.6. Peak Bed Temperature Variation with V_s

Figure 11 shows the peak bed temperature variation with superficial velocity from the current work; data are obtained from Fatehi and Kaviany (1994) and Saastamoinen et al. (2000) along with the equilibrium temperature corresponding to the overall equivalence ratio (at a given V_s). The equilibrium temperature was obtained using NASA SP-272 CEA. Temperature data from other works referred to earlier were discarded because of the use of K-type thermocouple, which can measure only up to 1500 K.

Experimental data obtained from the current study and from that of Fatehi and Kaviany (1994) show a monotonic increase in temperature with increase in superficial velocity and match closely with the semi-empirical predictions of Saastamoinen et al. (2000).

The temperatures measured go up to as high as 1850 K at $V_s = 0.25$ m/s ($\phi = 0.63$). The measured data show a linear variation of T_{pb} with V_s and ϕ; it gets increasingly close to equilibrium values with increasing V_s. This is essentially due to the fact that with increasing ϕ, thermochemical conversion process leads to reduced fraction of complex compounds (tars) thereby reducing the residence time to reach equilibration. This is in fact supported indirectly by the experimental data on composition (Figure 7), which shows that CH_4 fraction comes down significantly with increasing ϕ. Methane fraction of less about 1.5% ensures minimal higher hydrocarbons (see Dasappa et al., 2003). This result allows us to conclude that for $\phi > 0.4$, one can use equilibrium calculations to obtain T_{pb}.

5. RESOLUTION OF PERCEIVED DIFFERENCES IN PROCESS BEHAVIOR

It is now possible to clarify the differences in the perception of the bed behavior expressed in Porteiro et al. (2010a), Fatehi and Kaviany (1994), and Ronnback et al. (2001). The depiction of reaction limitedness for V_s between 17 and 38 cm/s is incorrect, because as seen from Figure 7, it is O_2 limited. In fact, O_2 drops to 0% in one particle depth in an operating bed, as can be noted from Figure 8. Volatile oxidation in diffusion flame mode dominates for $V_s < 16$ cm/s and char surface oxidation

dominates for $V_s > 16\,\text{cm/s}$. Since both these processes are diffusion controlled, regimes I and II have the same behavior, namely O_2 limitedness.

The depiction of Ronnback et al. (2001) that regime I is substoichiometric with $O_2 \neq 0$ is incorrect, as it is in conflict with the data on O_2 discussed just above. The reason for their conclusion was inferred from their description of the experimental procedure. Their data is sampled over 4 min. This is in fact close to the response time of the analyzer. If sufficient time for the measurements to become steady had been allowed, they would have also observed zero oxygen fraction. Hence, regime I and II are essentially fuel-rich, O_2-limited regimes. The depiction by Fatehi and Kaviany (1994) is indeed correct. Finally, Gort (1995) defines another term called partial gasification to connote regime I where some char will remain unconsumed. This is consistent with the experimental observation (see Figure 6), but to emphasize the importance of char reduction reactions, this regime is best termed *gasification*.

6. MODEL FOR FLAME PROPAGATION

The heat balance for a fresh biomass particle immediately upstream of the reaction zone can be written as,

$$mc_p \frac{dT_p}{dt} = A\left(f\epsilon\sigma\left(T_s^4 - T_p^4\right) - h(T_p - T_0)\right) \tag{2}$$

where m is the mass of the particle assumed spherical here (diameter d) and T_0 is the free stream temperature. The term due to particle temperature, T_p^4, is very small compared to T_s^4 and is ignored. The time for ignition can be calculated by integrating the equation from $T_p = 300K$ (ambient temperature) to $T_p = T_{ign}$. The resulting expression is

$$\dot{r} = \frac{d}{t_{ign}} = \frac{6\,h}{\rho_b c_p ln(\frac{1}{1-z})} \tag{3}$$

where $\dot{r}$ is the flame propagation rate, ρ_b is the packed bed density, $z = h(T_p - T_0)/(f\epsilon\sigma T_s^4)$, and f is the view factor.

$$h = Nu\,k/d; \quad Nu = 2 + 0.9Re_{bed}^{0.5}; \quad Re_{bed} = V_s d/(\nu(1 - \phi_{bed})) \tag{4}$$

where Re_{bed} is the Reynolds number for a particle in the bed, ν is the kinematic viscosity, ϕ_{bed} is the void fraction, and k is the thermal conductivity of air. Eq. (3) requires T_s as an input. In the gasification regime ($V_s < 16 \pm 1\,\text{cm/s}$), the devolatilizing layer of biomass is surrounded by a gas-phase diffusion flame, and T_s is obtained from the energy balance at the surface of this particle; it relates the regression rate Reynolds number to the difference between heat release and radiant heat loss. Drawing from Mukunda et al. (2007), the heat balance equation for the surface due to flow past it [see Eq. (5)] is written as

$$\frac{\epsilon\sigma\left(T_s^4 - T_0^4\right)}{\left[\frac{\mu c_p}{d_0}\right](T_s - T_0)} = (B-1)\frac{Nu}{Nu_0}Nu_0 \tag{5}$$

where,

$$B = \frac{H_v Y_{ox,0}}{s_v c_p (T_s - T_0)} \tag{6}$$

H_v is the caloric value of the volatiles (14 MJ/kg) and s_v is the stoichiometric coefficient (3.6). $Nu/Nu_0 = 0.7B^{0.75}$ (see Mukunda et al., 2007; Paul et al., 1982), takes into account the change in Nusselt number caused by outflowing gases from the surface, the so-called blocking effect. By solving Eq. (5) for T_s iteratively with a trial-and-error procedure assuming $Nu_0 = 2 + 0.9Re_{bed}^{0.5}$, we obtain a set of results for T_s that shows dependence on Nu_0. These data are curve-fitted by preserving the scaling quantity $(\mu c_p/d_0\epsilon\sigma)$ to lead to $T_s = (\mu c_p/d\epsilon\sigma)^{1/3} Nu_0^{0.36} = 482[K]Nu_0^{0.36}$; the properties are chosen at 600 K and char emissivity value of 0.85. The theoretical results are shown along with the experimentally determined T_s in Figure 9. The model results deviate from the experimental results by less than 5%. For $V_s > 16$ cm/s, T_s is taken from equilibrium calculations (see Figure 11).

6.1. Ignited Mass and Choice of Ignition Temperature

As was discussed earlier, in the gasification-dominated regime up to $V_s = 17$ cm/s, fresh biomass devolatilizes due to heat transfer from the hot char layer above it; the volatiles coming out mix with the incoming air and burn around the devolatilizing particle in diffusion-flame mode. Ignition essentially occurs in the gas phase, and further heat for devolatilization is supplied by the surrounding flame similar to single particle combustion. Therefore the mass of fresh biomass that needs to be heated for ignition is very small compared to the mass of a fresh biomass particle. Consistent with this observation, Eq. (3) overpredicted the propagation rate by six times. So the mass to be heated for ignition of gas phase flame is significantly smaller, perhaps one-sixth the mass of the particle, and once the gas-phase flame is established, further devolatilization occurs by heat transfer from the flame to the biomass particle. This also implies that the ignition temperature that must be used in Eq. (3) should correspond to the gas-phase ignition temperature of volatiles, which is around 650 K (see Quintiere, 2006). Therefore in the calculations, the numerical factor 6 in Eq. (3) is dropped and 650 K is used for the ignition temperature.

But for $V_s > 17$ cm/s, as was shown earlier, the gas-phase flame gets blown off from around the devolatilizing particle; the volatiles coming out get convected upward and burn around the hot char particle, leading to simultaneous oxidation of volatiles and char. Therefore the entire fresh biomass gets heated only because of heat transfer by radiation from the hot char on top until the surface reaches temperature sufficient for the char oxidation reactions to begin. So the mass to be heated for ignition in this case is very close to the mass of a fresh biomass particle, and the ignition temperature is that of the char, around 850 K. Another factor that must be taken into account once the char starts to oxidize is the formation of ash layer on the char surface, which will alter the emissivity. This aspect is dealt with in the following section.

6.2. Role of Ash on the Propagation Behavior

The source of ignition for flame propagation is radiation from the hot char surface just above the fresh biomass. The emissivity can be chosen to be close to unity (say 0.85) up to $V_s = 16\,\text{cm/s}$ as the char surface is not covered by ash. But beyond 16 cm/s, as discussed earlier, char oxidation starts to dominate, and the ash formed stays on the surface of the char (see Varunkumar et al., 2011). In the case of single char particles burning under ambient conditions, the ash layer plays a dual role. It brings down the heat loss from the surface by bringing down the emissivity as well as the surface temperature and adds an extra resistance to the transport of O_2 to the surface of the char, thereby establishing a delicate balance between convection and radiation (see Varunkumar et al., 2011). But in a packed bed, for $V_s > 18\,\text{cm/s}$, the temperature drop across the ash layer is taken as negligible; the ash layer brings down the effective emissivity at which the particles emit radiation to the fresh biomass or char. The emissivity data for the hot ash layer are obtained from the work of Wall et al. (1993) and Zbogar et al. (2005) on coal combustion in boilers. The emissivity is shown to decrease with an increase in temperature; also it is shown in Wall et al. (1993) that the fraction of radiation transmitted through a 0.4-mm-thick ash layer is just 5% and through a 1-mm-thick layer is less than 1%. Therefore, in the present model, the ash layer is assumed to be opaque and radiate at T_s with the emissivity correlation given in Zbogar and Frandsen (2003), as $\epsilon(T_s) = 1 - aT_s$, where $a = 0.0004[K^{-1}]$. This expression is extrapolated up to 2200 K.

Figure 12 shows the model results along with the emissivity data used; experimental data points are also shown. Uncertainty of 10% in the emissivity data leads to predictions that encompass most of the experimental data. The agreement between the model results and experiments is indeed good and clearly brings out the universal behavior of flame propagation through a packed bed of biomass. Measurements of $\dot{r}$ with steel and glass reactor are within 5% up to 50 cm/s; beyond 50 cm/s, it drops sharply leading to extinction in the glass reactor at ~55 cm/s and in the insulated steel reactor at ~65 cm/s. These imply that heat loss is the key factor initiating the extinction process. Further physical examination and videos show that extinction starts locally in some region near the wall and spreads around. This is understood as

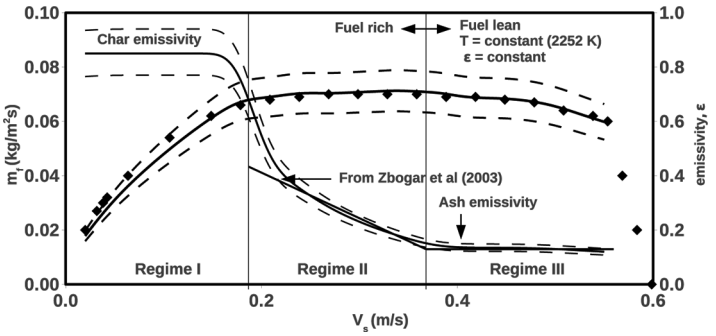

Figure 12 Model results. Solid line: model results; dashed lines: fuel mass flux calculated by incorporating ±10% uncertainty in emissivity; data points: experimental results; emissivity values with bounds and correlation of Zbogar and Frandsen (2003) are also shown.

follows. The combined effects of (a) enhanced voidage near the wall, (b) sharp local increase in velocity due to bed adjustment, and (c) reactive heating of the incoming stream lead to high local velocities of 2.5–3 m/s. This causes ash local blow off, enhanced radiation loss, and cooling-off (Varunkumar et al., 2011). This spreads around leading to overall extinction.

7. CONCLUSIONS

This article has addressed the processes in the thermochemical conversion of a packed bed of biomass particles. There have been various perceptions of the conversion process, mostly arising out of inadequate exploration of crucial thermochemical behavior. The data on exit gas composition and the change in O_2 fraction through the bed are used to show that the operation is substoichiometric over a large range of V_s (up to 40 cm/s). Visual examination of thin gaseous flames between particles and their flame temperatures close to the adiabatic flame temperature for the volatiles (1600 K) over a range of V_s up to 18 cm/s are taken to indicate the diffusion limitedness of the process; in this regime, the surface temperature is less than the gas phase temperature. For $V_s > 18$ cm/s, the difference between T_s and T_g vanishes due to simultaneous volatile and char oxidation processes. Based on these observations, two regimes of operation are identified, namely, gasification-reaction dominated ($V_s < 16 \pm 1$ cm/s) and char-oxidation dominated ($V_s > 16 \pm 1$ cm/s). In both these regimes, λ sensor data shows that O_2 drops from 21% to near 0% within one particle depth, confirming fast chemistry and transport limited dynamics. These inputs are used to develop a model that considers the thermal evolution of fresh biomass from ambient to ignition conditions. In the gasification regime, it is coupled with the surface heat balance equation for the flaming particle above the fresh biomass, and the predicted propagation rates match excellently with the experimental results. In the char oxidation regime, ash plays an important role in regulating the radiant heat transfer to the fresh biomass; and the variation of ash emissivity is shown to be crucial in explaining the observed behavior. In this regime also, the agreement between model results with experiments is shown to be very good. Finally, the observed variation of fuel consumption rate with air flow rate is shown to follow an universal trend irrespective of the biomass used; it is important to realize that this is primarily a consequence of diffusion limitedness of the conversion process.

REFERENCES

Collazo, J., Porteiro, J., Patiño, D., and Granada, E. 2012. Numerical modeling of the combustion of densified wood under fixed-bed conditions. *Fuel*, **93**, 149–159.

Cooper, J., and Hallett, W. 2000. A numerical model for packed-bed combustion of char particles. *Chem. Eng. Sci.*, **55**(20), 4451–4460.

Dasappa, S., Sridhar, H.V., Sridhar, G., Paul, P.J., and Mukunda, H.S. 2003. Biomass gasification—a substitute to fossil fuel for heat application. *Biomass Bioenergy*, **25**(6), 637–649.

Dosanjh, S.S., Pagni, P.J., and Fernandez-Pello, C. 1987. Forced cocurrent smoldering combustion. *Combust. Flame*, **68**, 131–142.

Fatehi, M., and Kaviany, M. 1994. Adiabatic reverse combustion in a packed bed. *Combust. Flame*, **99**, 1–17.

Gnanendra, P., Ramesha, D., and Dasappa, S. 2012. Preliminary investigation on the use of biogas sludge for gasification. *Int. J. Sustainable Energy*, **31**(4), 251–267.

Gort, R. 1995. On the propagation of a reaction front in a packed bed: thermal conversion of municipal waste and biomass. PhD thesis, University of Twente.

Gort, R., and Brouwers, J.J.H. 2001. Theoretical analysis of the propagation of a reaction front in a packed bed. *Combust. Flame*, **124**, 1–13.

Horttanainen, M., Saastamoinen, J., and Sarkomaa, P. 2002. Operational limits of ignition front propagation against airflow in packed beds of different wood fuels. *Energy Fuels*, **16**, 676–686.

Johansson, R., Thunman, H., and Leckner, B. 2007. Influence of intraparticle gradients in modeling of fixed bed combustion. *Combust. Flame*, **149**, 49–62.

La Fontaine, H., and Reed, T. 1993. An inverted downdraft wood-gas stove and charcoal producer. In Klass, D. (Ed.) *Energy from Biomass and Wastes*, volume XV, Institute of Gas Technology, Chicago.

Mukunda, H.S., Basani, J., Shravan, H.M., and Philip, B. 2007. Smoldering combustion of "incense" sticks, experiments and modeling. *Combust. Sci. Technol.*, **179**, 1113–1129.

Mukunda, H.S., Dasappa, S., Paul, P.J., Rajan, N.K.S., Yagnaraman, M., Kumar, D.R., and Deogaonkar, M. 2010. Gasifier stove—science, technology and outreach. *Curr. Sci.*, **98**(5), 627–638.

Paul, P.J., Mukunda, H.S., and Jain, V.K. 1982. Regression rates in boundary layer combustion. *Proc. Combust. Inst.*, **19**, 717–729.

Porteiro, J., Patino, D., Collazo, J., Granada, E., Moran, J., and Miguez, J. 2010a. Experimental analysis of the ignition front propagation of several biomass fuels in a fixed-bed combustor. *Fuel*, **89**(1), 26–35.

Porteiro, J., Patino, D., Moran, J., and Granada, E. 2010b. Study of a fixed-bed biomass combustor: Influential parameters on ignition front propagation using parametric analysis. *Energy Fuels*, **24**(7), 3890–3897.

Quintiere, J. 2006. *Fundamentals of Fire Phenomena*. Wiley Online Library, New york.

Reed, T., Walt, R., Ellis, S., Das, A., and Deutch, S. 1999. Superficial velocity—the key to downdraft gasification. In *Fourth Biomass Conference of the Americas*, Oakland, CA; Pergamon Press, Oxford, UK, pp. 343–356.

Ronnback, M., Axell, M., Gustavsson, L., Thunman, H., and Leckner, B. 2001. Combustion processes in a biomass fuel bed—Experimental results. In *Progress in thermochemical biomass conversion*. Wiley, New york.

Ryan, J., and Hallett, W. 2002. Packed bed combustion of char particles: Experiments and an ash model. *Chem. Eng. Sci.*, **57**(18), 3873–3882.

Ryu, C., Yang, Y., Khor, A., Yates, N., Sharifi, V., and Swithenbank, J. 2006. Effect of fuel properties on biomass combustion: Part I. Experiments–fuel type, equivalence ratio and particle size. *Fuel*, **85**(7–8), 1039–1046.

Saastamoinen, J., and Richard, J.-R. 1996. Simultaneous drying and pyrolysis of solid fuel particles. *Combust. Flame*, **106**(3), 288–300.

Saastamoinen, J.J., Taipale, R., Horttanainen, M., and Sarkomaa, P. 2000. Propagation of ignition front in beds of wood particles. *Combust. Flame*, **123**, 214–226.

Saastamoinen, J.J., Horttanainen, M., and Sarkomaa, P. 2001. Ignition wave propagation and release of volatiles in beds of wood particles. *Combust. Sci. Technol.*, **165**(1), 41–60.

Thunman, H., and Leckner, B. 2005. Influence of size and density of fuel on combustion in a packed bed. *Proc. Combust. Inst.*, **30**, 2939–2946.

Thunman, H., Davidsson, K., and Leckner, B. 2004. Separation of drying and devolatilization during conversion of solid fuels. *Combust. Flame*, **137**(1–2), 242–250.

Varunkumar, S., Rajan, N.K.S., and Mukunda, H.S. 2011. Single particle and packed bed combustion in modern gasifier stoves—density effects. *Combust. Sci. Technol.*, **183**(11), 1147–1163.

Wall, T., Bhattacharya, S., Zhang, D., Gupta, R., and He, X. 1993. The properties and thermal effects of ash deposits in coal-fired furnaces. *Prog. Energy Combust. Sci.*, **19**(6), 487–504.

Yang, Y., Sharifi, V., and Swithenbank, J. 2004. Effect of air flow rate and fuel moisture on the burning behaviours of biomass and simulated municipal solid wastes in packed beds. *Fuel*, **83**(11–12), 1553–1562.

Zbogar, A., and Frandsen, F. 2003. Surface emissivity of coal ashes. *IFRF Combustion Journal, (Article No 200305)*, 1–5.

Zbogar, A., Frandsen, F., Jensen, P., and Glarborg, P. 2005. Heat transfer in ash deposits: A modelling tool-box. *Prog. Energy Combust. Sci.*, **31**(5–6), 371–421.